

# Mechanism of Water Augmentation During IR Laser Ablation of Dental Enamel

Daniel Fried, PhD,<sup>1\*</sup> Nahal Ashouri, DDS,<sup>2</sup> Thomas Breunig, PhD,<sup>1</sup> and Ramesh Shori, PhD<sup>3</sup>

<sup>1</sup>Department of Preventive and Restorative Dental Sciences, University of California, San Francisco, San Francisco, California 94143

<sup>2</sup>Department of Growth and Development, University of California, San Francisco, San Francisco, California 94143

<sup>3</sup>Department of Electrical Engineering, University of California, Los Angeles, Los Angeles, California 90095

**Background and Objectives:** The mechanism of water augmentation during IR laser ablation of dental hard tissues is controversial and poorly understood. The influence of an optically thick applied water layer on the laser ablation of enamel was investigated at wavelengths in which water is a primary absorber and the magnitude of absorption varies markedly.

**Study Design/Materials and Methods:** Q-switched and free running Er: YSGG (2.79  $\mu\text{m}$ ) and Er:YAG (2.94  $\mu\text{m}$ ), free running Ho:YAG and 9.6  $\mu\text{m}$  TEA CO<sub>2</sub> laser systems were used to produce linear incisions in dental enamel with and without water. Synchrotron-radiation IR spectromicroscopy with the Advanced Light Source at Lawrence Berkeley National Laboratory was used to determine the chemical changes across the laser ablation profiles with a spatial resolution of 10- $\mu\text{m}$ .

**Results:** The addition of water increased the rate of ablation and produced a more desirable surface morphology during enamel ablation with all the erbium systems. Moreover, ablation was markedly more efficient for Q-switched (0.15 microsecond) versus free-running (150 microsecond) erbium laser pulses with the added water layer. Although the addition of a thick water layer reduced the rate of ablation during CO<sub>2</sub> laser ablation, the addition of the water removed undesirable deposits of non-apatite mineral phases from the crater surface. IR spectromicroscopy indicates that the chemical composition of the crater walls deviates markedly from that of hydroxyapatite after Er:YAG and CO<sub>2</sub> laser irradiation without added water. New mineral phases were resolved that have not been previously observed using conventional IR spectroscopy. There was extensive peripheral damage after irradiation with the Ho:YAG laser with and without added water without effective ablation of enamel.

**Conclusions:** We postulate that condensed mineral phases from the plume are deposited along the crater walls after repetitive laser pulses and such non-apatitic phases interfere with subsequent laser pulses during IR laser irradiation reducing the rate and efficiency of ablation. The ablative recoil associated with the displacement and vaporization of the applied water layer removes such loosely adherent phases maintaining efficient ablation during multiple pulse irradiation. *Lasers Surg. Med.* 31:186–193, 2002. © 2002 Wiley-Liss, Inc.

**Key words:** erbium laser; CO<sub>2</sub> laser; dental enamel; laser ablation; infrared spectromicroscopy

## INTRODUCTION

It has been well established that extensive water application is necessary for the efficient ablation of dental hard tissues with Er:YAG and Er:YSGG laser irradiation. The mechanism of interaction between the water-layer, the laser radiation, and the hard tissues is not clearly understood and is somewhat controversial. Early mechanistic studies focused on tissue dehydration [1–4]. However, water absorption and diffusion studies in enamel indicate that only approximately half of the water is actually diffusible [5] and the rate for water diffusion is quite slow, on the order of several hours to days. Thermal analysis studies indicate that the tissue has to be heated to temperatures exceeding 200–300°C before the diffusible water is removed [6]. Higher temperatures of up to 800°C are required to remove the more tightly bound water [6]. Therefore, it is unlikely that simple dehydration by diffusion has a significant effect during laser irradiation.

Other more novel hypotheses include cavitation bubbles, accelerated water droplets, and apatite crystalline fragments. One proposed mechanism dubbed the “hydrokinetic effect” suggests that water droplets are rapidly accelerated into the enamel by absorption in the laser beam [7,8]. Altshuler et al. [9,10] have proposed that solid particles of ablated material are accelerated against the walls of the crater resulting in a polishing effect that removes debris and any protruding sharp edges. In the same study, the authors found that the ablation of enamel could be effectively enhanced by a factor of four via ablation with a quartz or sapphire contact-mode fiber during the initial few laser pulses. Solid particles were reflected by the fiber tip and particles originated from failure of the fiber.

Grant sponsor: NIH/NIDCR; Grant numbers: ROI-DE14554, R29-DE12091, T35-DE07103; Grant sponsor: DOE; Grant number: DE-AC03-76SF00098.

\*Correspondence to: Daniel Fried, PhD, Department of Preventive and Restorative Dental Sciences, University of California, San Francisco, 707 Parnassus Ave., San Francisco, CA 94143. E-mail: dfried@itsa.ucsf.edu

Accepted 7 May 2002  
Published online in Wiley InterScience  
(www.interscience.wiley.com).  
DOI 10.1002/lsm.10085

Majaron et al. [11] found that if the fiber was placed in a water droplet, there was a critical distance at which ablation was enhanced.

Poorly crystalline fused enamel particles and any surface protrusions or asperities formed in the ablation crater during the initial laser pulses are likely to inhibit efficient ablation for subsequent laser pulses leading to stalling and excessive heat accumulation. Even if the forces imparted to the enamel surface by laser-irradiated recoiling water particles may not be sufficient to ablate the normal intact enamel, they may be sufficient to cleanse the surface of loosely attached melted or recondensed mineral after the preceding laser pulses. These same forces result in the cavitation of the water layer [12–14] and energetically propel the remaining water on the surface several centimeters from the tooth. Zeck et al. [15] identified areas with a “white-chalky appearance which he labeled crystallites” that were particularly evident during scanning ablation with Er:YAG lasers when water was not used as a coolant. In addition, Rechmann et al. [16] have shown that when troughs that cuts were made in dental enamel without a water spray, there was a loosely attached layer of fused enamel. Such a layer would most certainly be water deficient and would be more resistant to ablation with Er:YAG laser pulses.

In this study, we compared the effect of an applied water layer on the depth of cut and crater surface morphology after multiple pulse irradiation for several clinically relevant IR laser systems in which the degree of absorption in water and mineral varied markedly (Table 1). The effect of the pulse duration on water augmented ablation was investigated by comparing Q-switched (0.15-microsecond) and free running (150-microseconds) erbium laser pulses. The associated mechanical forces important in the mechanism of water augmentation should be more pronounced for shorter laser pulses that produce greater recoil forces and stress transients. Previous studies of dental hard tissue ablation using Q-switched Er:YAG laser pulses indicated that stalling during multiple pulse ablation manifested a very strong dependence on a surface film of water applied to the surface of the enamel samples [17].

During high intensity laser irradiation, marked chemical and physical changes may be induced in the irradiated dental enamel. These changes can have profound effects on the laser ablation/drilling process leading to a reduction in the ablation rate and efficiency, increase in peripheral thermal damage, and even lead to stalling without further removal of tissue with subsequent laser pulses. Moreover, thermal decomposition of the mineral can lead to changes in the susceptibility of the modified mineral to organic acids in the oral environment. Morphological changes may also result in the formation of loosely attached layers of modified enamel that can delaminate leading to failure during the bonding to restorative materials [16,18]. Therefore, it is important to thoroughly characterize the laser (thermal) induced chemical and crystalline changes after laser irradiation. The mineral, hydroxyapatite, found in bone and teeth contains carbonate inclusions that render it highly susceptible to acid dissolution by organic acids generated from bacteria in dental plaque. Upon heating to

temperatures in excess of 400°C, the mineral decomposes to form a new mineral phase that has increased resistance to acid dissolution [19–22]. Recent studies suggest that as a side effect of laser ablation, the walls around the periphery of a cavity preparation will be transformed through laser heating into a more acid resistant phase with an enhanced resistance to future decay [23–25]. However, poorly crystalline non-apatite phases of calcium phosphate may have an opposite effect on plaque acid resistance [21] and may increase the quantity of poorly attached grains associated with delamination failures.

IR spectroscopy has been used for half a century to study the structure of bony tissue [26–28]. Fowler and Kuroda [20,21] used IR transmission spectroscopy to show the chemical changes induced in laser-irradiated dental enamel. Featherstone et al. [29] showed that the amount of carbonate in synthetic carbonated hydroxyapatites could be quantified using IR transmission measurements. The method employed by the aforementioned investigators was to grind away the surface of the irradiated enamel and mix it with KBr to produce a pellet. A limitation with that procedure is that it is never clear whether the powder used in the KBr pellet is contaminated by the underlying normal enamel substrate since the modified layer of laser-irradiated enamel is typically only a few microns thick. FTIR spectroscopy in specular reflectance mode is better suited for non-destructively resolving chemical changes on the surface of enamel [30]. The principal advantage of this technique is that the tissue reflectance is only influenced by a surface layer of a thickness on the order of the wavelength of the light. Thus, surface changes localized to the outer 10  $\mu\text{m}$  of tissue are probed. In previous studies, the area of the carbonate bands at 1400  $\text{cm}^{-1}$  were correlated with the transformation of mineral phase to a more acid resistant phase of hydroxyapatite with a marked reduction in the dissolution rate [30]. The incident fluence that was sufficient to induce loss of carbonate in the FTIR spectra coincided with the optimum laser fluence that inhibited both surface and subsurface acid dissolution. Therefore, FTIR spectroscopy is useful as a non-destructive probe to elucidate the optimum laser parameters to inhibit acid dissolution. This technique, however, requires smooth surfaces of large area in order to acquire suitable spectra. Spatial resolutions of 10  $\mu\text{m}$  can be achieved across rough ablation craters using a high brightness diffraction limited beam of IR synchrotron radiation. In this study, using Synchrotron Radiation-FTIR (SR-FTIR), we were able to non-destructively probe specific areas of these ablation craters and resolve the laser-induced chemical changes in the mineral phase. The SR-FTIR spectra presented in this study indicate that the chemical composition of those fused areas “crystallites” in the craters deviates markedly from that of hydroxyapatite.

## MATERIALS AND METHODS

### Laser Parameters

Blocks of bovine enamel were irradiated using Ho:YAG (2.1  $\mu\text{m}$ ), Er:YSGG (2.79  $\mu\text{m}$ ), Er:YAG (2.94  $\mu\text{m}$ ), and CO<sub>2</sub>

(9.6  $\mu\text{m}$ ) laser systems. The  $\text{CO}_2$  laser is a long-pulse TEA  $\text{CO}_2$  laser with a pulse duration of 6–8 microseconds from Argus Photonics Group (Jupiter, FL). The solid state Schwartz 123 laser systems were manufactured by Schwartz Electro-Optics (Orlando, FL) and were modified for more efficient diffuse pumping. A rotating mirror Q-switch was used to produce the short Er:YAG and Er:YSGG laser pulses of 150-nanoseconds duration. The respective absorption coefficients and depth of absorption in both water and enamel is tabulated for each laser wavelength employed in this study in Table 1.

The laser energy was measured and calibrated using laser calorimeters, Model ED-200 Gentec (Quebec, Canada). Two dimensional images of the respective laser spatial profiles were acquired using a Pyrocam I pyroelectric array from Spirocon (Logan, UT). The beam diameter at the position of irradiation was measured by scanning with a razor blade across the beam. The spot profile was single mode and fluences were defined using a Gaussian beam with a  $1/e^2$  beam diameter.

### Tissue Irradiation

Longitudinal cuts approximately 3-mm long and 200–300  $\mu\text{m}$  wide were produced on the enamel surface of  $5 \times 5 \text{ mm}^2$  blocks that were prepared from extracted bovine incisors, and polished to a 1- $\mu\text{m}$  finish. Two incisions were made at each fluence, one with and one without a layer of water. There were 20 laser pulses per spot with overlapping laser spots separated by 50  $\mu\text{m}$  to ensure a smooth intensity profile longitudinally through the incision. The procedure is illustrated in Figure 1. The bovine block was scanned using a computer controlled motion control system ESP 300 Newport (Irvine, CA) with an X-Y stage. Droplets of water were manually applied to the ablation site before each sequence of five laser pulses using a pipette with a volume of 5  $\mu\text{l}$ . The 5- $\mu\text{l}$  droplets were 950- $\mu\text{m}$  thick at the center with a diameter of 3 mm. After surface ablation, the lateral incisions were examined with an Olympus BX-50 microscope, Olympus America (Melville, NY) with a maximum magnification of 500 times interfaced to a high-resolution digital camera DVC 1300C DVC Company, Inc (Austin, TX). Measurements of incision depth and width were made with calibrated image analysis software, Image Pro Plus image analysis software, Media Cybernetics (Silver Spring, MD), that is

**TABLE 1. Absorption Coefficients in Water and Enamel for Each Laser Wavelength Employed in This Study Are Tabulated in the Table Below [37–39]**

Laser wavelength	Absorption coefficient in $\text{H}_2\text{O}$ (absorption depth*)	Absorption coefficient in enamel (absorption depth*)
2.1 $\mu\text{m}$	$25 \text{ cm}^{-1}$ (400 $\mu\text{m}$ )	$< 5 \text{ cm}^{-1}$
2.79 $\mu\text{m}$	$6,500 \text{ cm}^{-1}$ (1.6 $\mu\text{m}$ )	$400 \text{ cm}^{-1}$ (25 $\mu\text{m}$ )
2.94 $\mu\text{m}$	$12,250 \text{ cm}^{-1}$ (0.8 $\mu\text{m}$ )	$800 \text{ cm}^{-1}$ (13 $\mu\text{m}$ )
9.6 $\mu\text{m}$	$590 \text{ cm}^{-1}$ (17 $\mu\text{m}$ )	$8000 \text{ cm}^{-1}$ (1.3 $\mu\text{m}$ )

\*depth at which intensity falls to  $(1/e)$  of initial intensity.

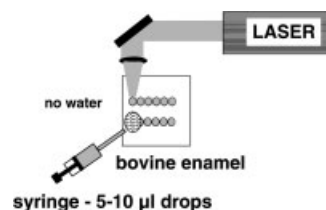


**Fig. 1.** The setup for producing lateral cuts in polished bovine enamel blocks. A syringe was used to manually apply a droplet of water before each five laser pulses.

capable of direct length and area. Several serial sections of approximately 100- $\mu\text{m}$  thickness were cut normal to the long axis of the incisions using a hard tissue microtome for polarized light microscopy (PLM). After cutting, sections were imbibed with water and viewed in the Olympus BX-50 microscope using crossed polarizers and a Red I waveplate. The wave-plate introduces a 530-nm phase retardation so that addition and subtraction colors introduced by the tissue birefringence induce resolvable changes in color. In the case of thermal changes, i.e., melting and recrystallization, loss of birefringence and increased attenuation of the illumination light causes altered tissue to appear black, which is easier to discern under polarized light.

### Infrared Spectromicroscopy (SR-FTIR)

A Nicolet Magna 760 FTIR interfaced to a Nic-Plan IR microscope, equipped with a motorized sample stage connected to beam-line 1.4.3 of the Advanced Light Source at Lawrence Berkeley National Laboratory was used to acquire spectra of the dental enamel irradiated with the  $\text{CO}_2$  laser [31]. Specular reflectance spectra were acquired with a spatial resolution of 10  $\mu\text{m}$  by scanning the 10  $\mu\text{m}$  spot imaged by the FTIR microscope across the laser intensity profile from the center of the laser incision to the normal enamel outside the incision.

### Collection of Condensed Mineral Phases From Plume

Ejected particles were collected on infrared transparent  $\text{BaF}_2$  substrates after ablation with the 9.6  $\mu\text{m}$  TEA  $\text{CO}_2$  laser in a high-vacuum system. The vacuum system, a 2.5-inch small-volume spherical chamber was pumped down to a microtorr using an EXC120 turbomolecular/diaphragm oil-free pumping station Edwards High Vacuum International (Crawley, West Sussex, UK). Ejected plume debris was collected at a  $45^\circ$  angle to the ejection axis (see Fig. 9).

## RESULTS

### Lateral Incisions With and Without Water

Lateral cuts were produced in the bovine blocks at irradiation intensities up to  $200 \text{ J/cm}^2$  using free running and Q-switched erbium laser pulses. When water was not used, the ablation craters were typically quite shallow and areas of fused enamel were clearly visible. After the application of a water layer of sufficient thickness, smooth craters, devoid of any fused areas of enamel were

produced. The craters were markedly deeper suggesting that the fused material observed upon ablation without the water presents inhibits further ablation. Shorter Q-switched laser pulses produced more uniform cuts through the water presents layer at markedly lower fluences than those required for efficient cutting using the longer erbium laser pulses. If no water layer was applied, ablation was not as efficient and areas of fused enamel were observed, see Figure 2c,d. Serial sections of 100- $\mu\text{m}$  thickness taken from the ablation craters and viewed under  $500\times$  magnification in polarized light show peripheral cracks and evidence of thermal damage when water was not used (Fig. 3). In contrast, uniform conical craters were produced with minimal thermal or acoustic damage (cracks) when water was applied before ablation. For Q-switched Er:YAG laser pulses smooth incisions were produced above fluences of  $40\text{ J/cm}^2$  while for the free-running Er:YAG fluences in excess of  $100\text{ J/cm}^2$  were required (see Fig. 4). We did not observe the peripheral damage that was observed in a previous study of Q-switched Er:YAG laser ablation [17] for larger spot sizes.

Similar results were observed for free running and Q-switched Er:YSGG laser pulses. The threshold for smooth cuts was  $28\text{ J/cm}^2$  for the Q-switched Er:YSGG laser and  $81\text{ J/cm}^2$  for the free-running Er:YSGG laser. There was a fivefold increase in the ablation depth at fluences exceeding  $20\text{ J/cm}^2$  with the added water layer before ablation during irradiation with the Q-switched laser pulses (see Fig. 4). At high irradiation intensities,  $>100\text{ J/cm}^2$ , a similar increase in rate was noted for the free running Er:YSGG laser pulses with the added water. The ablation depth versus incident fluence saturates between  $20\text{--}30\text{ J/cm}^2$  for Q-switched laser pulses due to plasma formation

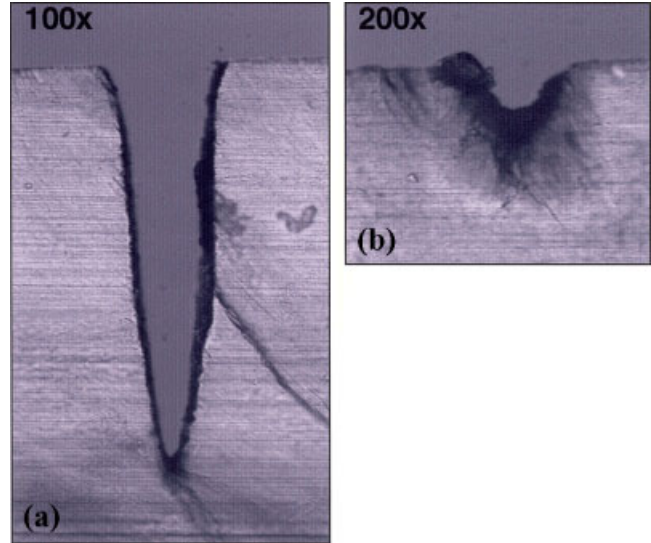


Fig. 3. Polarized light images of 100- $\mu\text{m}$  thick cross sections of the Q-switched Er:YAG laser cuts of Figure 2c,d with (a) and without (b) water. The respective crater dimensions are (a) 125- $\mu\text{m}$  across and 490- $\mu\text{m}$  in depth and (b) 33- $\mu\text{m}$  across and 52- $\mu\text{m}$  deep.

above the surface of the tooth. Absorption of the incident laser radiation in the plasma restricts the ablation rate [17,32] and the most efficient ablation occurred near the threshold for plasma formation.

Extensive damage to the mechanical integrity of the bovine block and thermal damage to the underlying dentin

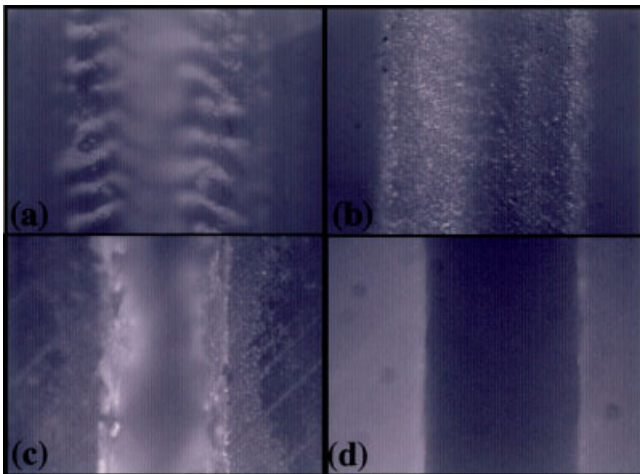


Fig. 2. Lateral cuts in the surface of polished bovine blocks using a  $9.6\text{ }\mu\text{m}$  TEA  $\text{CO}_2$  laser pulse with a fluence of  $70\text{ J/cm}^2$ , (a) no droplet added, (b) water added; and a Q-switched Er:YAG laser pulses with a fluence of  $15\text{ J/cm}^2$ , (c) no water added and (d) a water droplet placed before each five laser pulses.

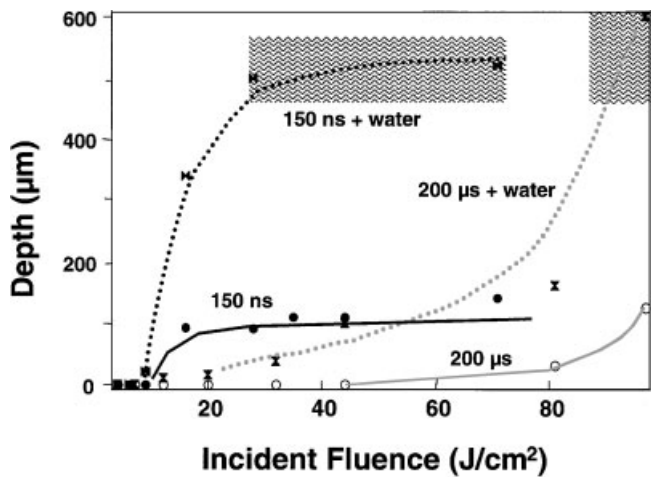


Fig. 4. The ablation depth at various irradiation intensities for the free-running (150 microseconds) and Q-switched (150 nanoseconds) Er:YSGG laser pulses with (dotted line) and without (solid line) the addition of water. The shaded regions represent the fluence range in which smooth lateral cuts were achieved similar to those of Figure 2d. Five laser pulses per spot, 300- $\mu\text{m}$  spot size and 50- $\mu\text{m}$  scan distance.

was observed after irradiation with the free running Ho:YAG laser at  $2.1\ \mu\text{m}$  (Fig. 5) even with a layer of water applied to the surface. Laser light at  $2.1\ \mu\text{m}$  is only weakly absorbed by water. Therefore, it is able to penetrate through that water layer without the transfer of much energy and through the outer 1–2-mm layer of enamel where it is absorbed by the dentin resulting in thermal damage. Monte Carlo simulations of light deposition in teeth followed by calculation of the subsequent temperature rise have predicted localized thermal damage at the dentin–enamel junction (DEJ) during Nd:YAG ( $1.064\ \mu\text{m}$ ) irradiation without ablation of the outer enamel [33]. Localized subsurface damage was visible at the DEJ after Ho:YAG irradiation. At higher incident fluence, thermal stresses generated at the DEJ produced large fractures transverse to the path of laser irradiation resulting in the destruction of the bovine enamel block. This result exemplifies the danger of irradiating teeth with free-running Nd:YAG and Ho:YAG laser pulses—even with extensive water spray.

During  $\text{CO}_2$  laser irradiation, particularly at  $9.6\ \mu\text{m}$ , absorption is an order of magnitude higher in the mineral than in the water (see Table 1). Therefore, we did not expect to observe a pronounced effect from the water layer. As we expected, the water reduced the depth of the ablation craters and the efficiency of ablation. However,

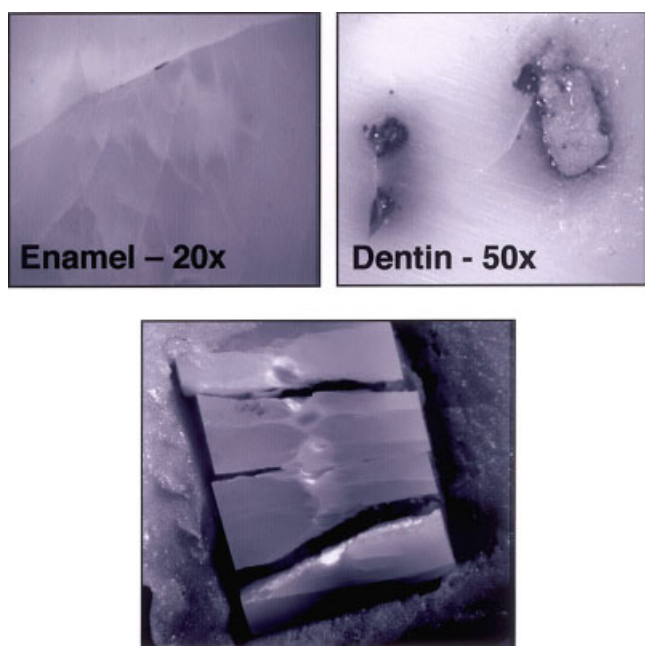


Fig. 5. Laser irradiated bovine blocks using a free-running Ho:YAG laser at  $2.1\ \mu\text{m}$  (**upper left**). Front surface of bovine block after laser pulses at  $70\ \text{J}/\text{cm}^2$ —no damage is visible on the enamel surface, however, subsurface dentin damage is visible (**upper right**). Dentin side of bovine block shows extensive charring of the dentin proteins (**bottom**). Higher incident fluences,  $150\ \text{J}/\text{cm}^2$ , result in extensive fractures transverse to the laser cut.

there were profound differences in the surface morphology of the ablation crater with and without the water layer (Fig. 2a,b).

Large uniform areas of the ablation crater were covered with fused enamel resembling a glazed or glassy surface when water was not used. In contrast, the surface morphology produced with the water is of uniform roughness and does not contain the glazed zones of enamel. SR-FTIR spectra from the ablation craters indicate that the fused or glazed zones contain non-apatite phases of the enamel mineral (see below). In contrast, with the water layer present the chemical composition of the mineral phase on the crater walls is a purer phase hydroxyapatite mineral with the removal of the carbonate defects.

### SR-FTIR

Spectra acquired from within different regions on the samples irradiated using TEA  $\text{CO}_2$  laser pulses with and without an applied water layer are shown in Figs. 6 and 7. The spectral series shown in Figure 6 was taken across the lateral incision shown in Figure 2a with a spatial resolution of  $10\text{-}\mu\text{m}$ . The marked differences of the spectra with position in the crater indicate that the chemical composition of the irradiated dental enamel varies markedly throughout the regions of the crater that were exposed to different laser intensity levels. In Figure 7, two spectra taken from the incisions shown in Figure 2a,b are compared with normal non-irradiated enamel. The first spectra of Figure 7a represents the normal enamel with the characteristic peaks due to the phosphate group in carbonated hydroxyapatite near  $1000\ \text{cm}^{-1}$  and two small peaks near  $1400\ \text{cm}^{-1}$  due to the carbonate group. The second spectrum of Figure 7a was taken  $60\ \mu\text{m}$  from the center of the crater (Fig. 2a) and it contains none of the bands representative of hydroxyapatite, tetra-calcium phosphate, or even tri-calcium phosphate phases. Some of the bands are more representative of lower order calcium

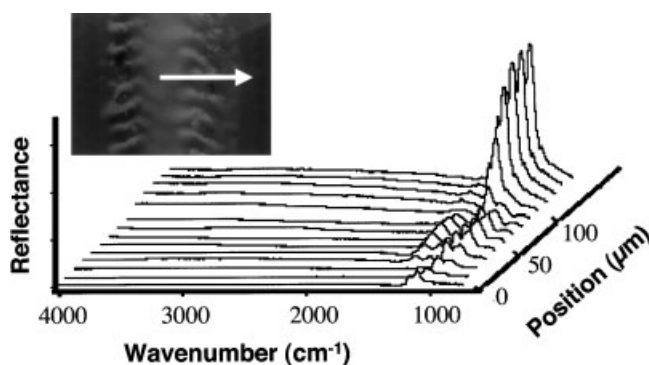


Fig. 6. (**Top left image**)  $\text{CO}_2$  laser produced incision in the surface of a bovine enamel block at a wavelength of  $9.6\ \mu\text{m}$ , pulse duration of 8 microseconds, and fluence of  $70\ \text{J}/\text{cm}^2$  without an added layer of water. SR-FTIR spectra were acquired with a spatial resolution of  $10\ \mu\text{m}$  from the center of the incision to the normal enamel. The spectra change markedly across the crater topography.

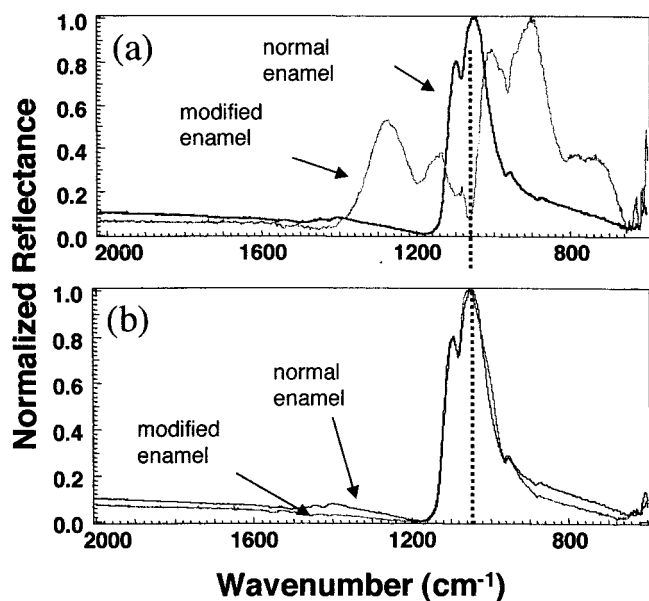


Fig. 7. SR-FTIR spectra taken of the lateral incisions produced using the CO<sub>2</sub> laser shown in Figure 2a (**top-a**) and Figure 2b (**bottom-b**) are indicated by gray dotted lines. Spectra of normal enamel are represented by the black solid line in each figure. The vertical dotted line at 1041 cm<sup>-1</sup> represents the laser wavelength. Note the shift in the absorption maxima in (a).

phosphates such as mono-calcium phosphate or calcium hydroxide which was observed by Aminzadeh et al. [34] using Raman spectroscopy after CO<sub>2</sub> laser irradiation. With the exception of Ca(OH)<sub>2</sub> these new bands, to our knowledge have not been previously observed after either the heat treatment or laser irradiation of dental hard tissues. However, these non-apatitic phases are likely to exhibit higher dissolution rates and be poorly attached to the underlying mineral. Figure 7b shows two spectra taken from an incision produced under the same conditions as the incision shown in Figure 2a with a droplet of water added before each sequence of five laser pulses. The first spectrum is of normal enamel and the second is taken from the center of the laser incision. We suspect that the added layer of water aids in preventing the formation of fused areas of the non-apatitic phases and results in a more desirable surface morphology. The modified enamel within the crater are lacking the two carbonate bands located near 1400 cm<sup>-1</sup>, indicative of the formation of the desired purer phase hydroxyapatite with fewer chemical defects [20,30,35].

Spectra were taken from the craters produced with and without water using the free-running Er:YAG laser at a fluence of 200 J/cm<sup>2</sup>. Non-apatite phases are apparent similar to tri- and tetra-calcium phosphates when water was not added, see Figure 8. In contrast, spectra acquired with the added water exhibit minimal changes, i.e., minor changes in the phosphate and carbonate bands, near 1000 and 1400 cm<sup>-1</sup>, respectively.

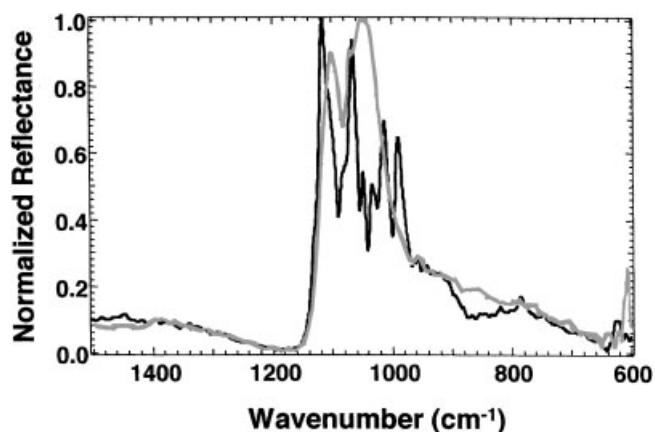


Fig. 8. Spectra of bovine enamel from the ablation crater produced by a free-running Er:YAG laser (200 J/cm<sup>2</sup>) with (gray line) and without (black line) an added water layer. The spectrum with added water is similar to that of unmodified enamel, while other phases are visible when water was not applied before ablation.

In order to test our hypothesis that non-apatite mineral phases are formed in the plume and are redeposited on the tissue surface, we collected material ejected from enamel during CO<sub>2</sub> laser ablation on IR transparent (BaF<sub>2</sub>) substrates in a vacuum. SR-FTIR and optical images of the particles are shown in Figure 9. Some of the spectral bands are similar to those of the secondary phases of Figure 7a produced under similar conditions suggesting that the origin of the CO<sub>2</sub> “recrystallites” is recondensation from the plume. The spectra acquired at erbium laser wavelengths are fundamentally different from Figure 7a and 9, and the mechanism of ablation differs from that of the carbon dioxide laser. Therefore, we postulate that there may be a different mechanism responsible for their formation.

## DISCUSSION

This study demonstrates that an applied water layer of sufficient thickness has a profound effect on ablation rate, ablation efficiency and the surface morphology of the crater walls. This is of particular importance for Q-switched erbium laser ablation in which the influence of the water layer on preventing stalling and excessive peripheral damage is apparently more pronounced. In previous studies investigating the efficiency of enamel and dentin ablation with Q-switched erbium laser pulses, it was difficult to assess the influence of water on the ablation process. It is probable that the water layer was not of sufficient thickness [17,32,36], that, it is much easier to assess the effect of the water layer on incisions produced on polished surfaces rather than on single ablation sites.

Based on the phenomenological observations of this study, we can provide some speculation about the mechanism of the water–enamel interaction. We can easily rule out the mechanism proposed by Rizoïu et al. [8], i.e., the hydrokinetic effect, in which water droplets in the water

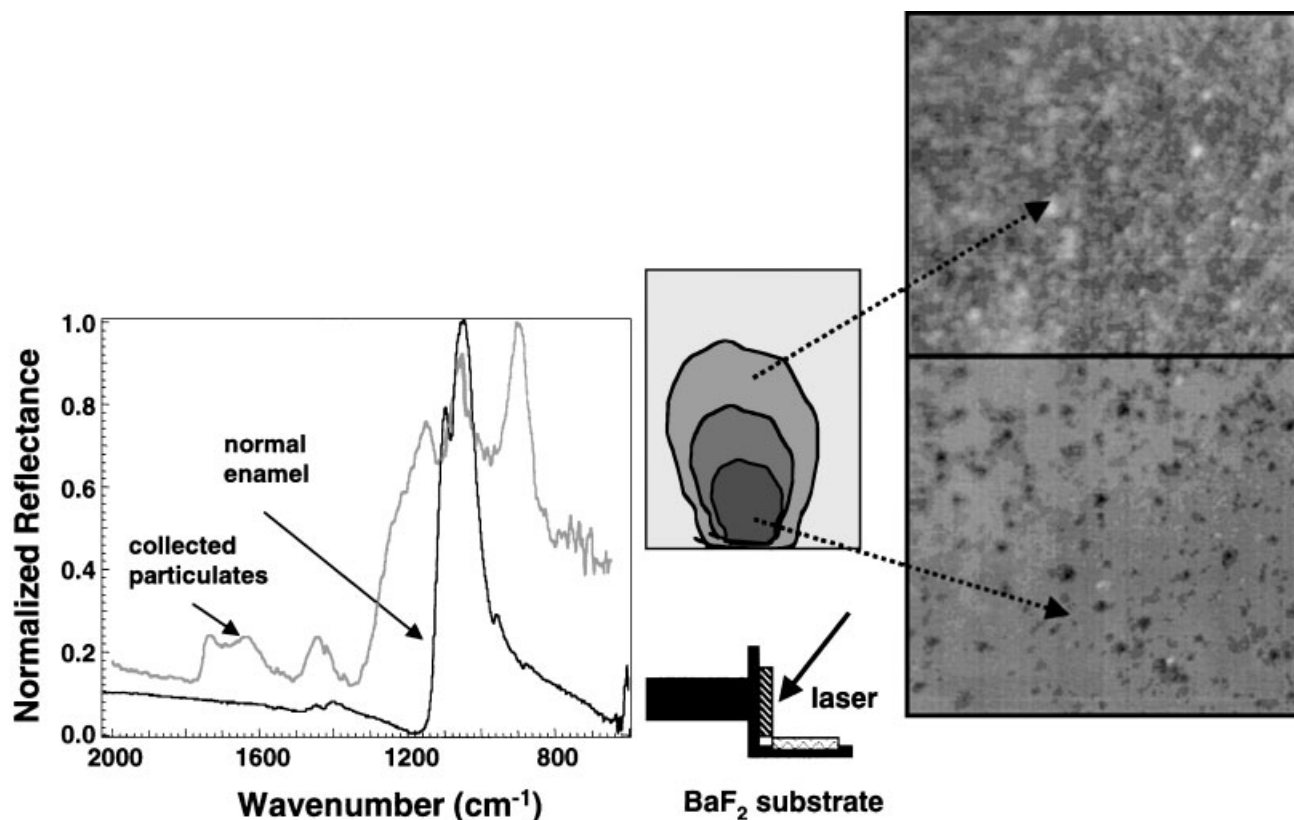


Fig. 9. Ejected particles collected in a vacuum system at 1- $\mu$ torr after ablation of enamel using a 9.6  $\mu$ m TEA CO<sub>2</sub> laser. The particles are deposited in a fan shaped distribution on a BaF<sub>2</sub> substrate. Optical images (320 $\times$ ) of the low density zone (**top**) and high density zone (**bottom**) are shown on the right. SR-FTIR spectra of the particles (gray) and normal enamel are shown on the left.

spray are accelerated by the laser photons, since there was no water spray, only a static water layer. Although the effect of secondary bombardment by particles and water droplets proposed by Altshuler [9] explains the smoother crater and higher ablation rate with the erbium laser pulses it does not explain the presence of fused/melted enamel with both CO<sub>2</sub> and erbium laser pulses and the decrease in ablation rate with CO<sub>2</sub> laser ablation. It is likely that the forces associated with strong absorption of the laser radiation in the water followed by the subsequent recoil of the water removes any poorly attached non-apatite phases of modified enamel that may adversely affect bonding and solubility, in addition to reducing the rate and efficiency of ablation.

There was an optimum fluence regime for both the free-running and Q-switched erbium laser pulses that produced smooth craters with the applied water layer, although the Q-switched ablation craters manifested less surface roughness than the free-running ablation craters. Dental enamel ablation for Q-switched Er:YAG and Er:YSGG laser pulses is markedly more efficient than for the free-running erbium laser pulses if a water layer of sufficient thickness is used. If the water layer is not sufficiently thick then ablation rapidly stalls after only a

few laser pulses leaving a fused layer of non-hydroxyapatite calcium phosphate phases. For long-pulse TEA laser pulses (6–8 microseconds) at 9.6  $\mu$ m the surface morphology was markedly different when a layer of water was used. Although the water layer reduced the efficiency of ablation, the resulting surface morphology was superior consisting of a purer hydroxyapatite with fewer chemical defects. In contrast, areas of the ablation crater produced without water contained areas of less desirable, non-apatite calcium phosphate phases.

Under the appropriate laser irradiation conditions, with an applied water layer, minor chemical and crystalline changes were observed in the enamel. These desirable changes are likely to be associated with higher bond strengths to restorative materials and increased resistance to acid dissolution [30,35]. Using SR-FTIR, we acquired well-resolved spectra from the rough surfaces of the interior of the ablation craters with a spatial resolution of 10  $\mu$ m. The spectra acquired after CO<sub>2</sub> and Er:YAG laser irradiation without water exhibit peaks between 700 and 1400  $\text{cm}^{-1}$  that have previously been unobserved after laser irradiation. Such non-apatite phases formed after ablation without water may potentially be more susceptible to acid dissolution and be loosely attached to the underlying

unaltered enamel substrate leading to poor bonding to restorative materials.

Future efforts will focus on elucidating the morphological and chemical nature of the material ejected or ablated from the enamel and the mechanism of particle formation.

## ACKNOWLEDGMENTS

This work was supported by an NIH/NIDCR research grants RO1-DE14554 and R29-DE12091. The ALS supported by DOE DE-AC03-76SF00098. Nahal Ashouri was supported by a NIH/NIDCR Newbrun Fellowship Grant T35-DE07103. The TEA CO<sub>2</sub> laser was provided by Argus Photonics Group. The authors gratefully acknowledge Michael Martin of LBL for his assistance at the ALS and John Featherstone, Charles Le, Larry Watanabe and John Xie for their contributions at UCSF.

## REFERENCES

- Vickers VA, Jacques SL, Schwartz J, Motamedi M, Rastegar S, Martin JW. 1992. Ablation of hard dental tissues with the Er:YAG laser. *Laser-Tissue Interaction III*, Vol. 1646:46-55 (SPIE, Los Angeles, 1992).
- Walsh JT, Hill DA. 1991. Erbium laser ablation of bone: Effect of water content. *Laser-Tissue Interaction II*, Vol. 1427:27-33 (SPIE, Los Angeles, 1991).
- Wigdor HA, Walsh JT, Visuri SR. 1994. Effect of water on dental material ablation of the Er:YAG laser. *Lasers in Surgery: Advanced Characterization, Therapeutics, and Systems IV*, Vol. 2128 (SPIE, 1994).
- Burkes EJ, Hoke J, Gomes E, Wolbarsht M. Wet versus dry enamel ablation by Er:YAG laser. *J Prosthet Dent* 1992;67:847-851.
- Dibdin GH. The water in human dental enamel and its diffusional exchange measured by clearance of tritiated water from enamel slabs of varying thickness. *Caries Res* 1993;27:81-86.
- Holcomb DW, Young RA. Thermal decomposition of human tooth enamel. *Calcif. Tissue Int* 1980;31:189-201.
- Rizoiu I, Kimmel AI, Eversole LR. The Effects of an Er, Cr:YSGG laser on canine oral tissues. *Laser Applications in Medicine and Dentistry*, Vol. 2922:74-83 (SPIE, 1996).
- Rizoiu I.M, DeShazer LG. 1994. New laser-matter interaction concept to enhance hard tissue cutting efficiency. *Laser-Tissue Interaction V*, Vol. 2134A:309-317 (San Jose, 1994).
- Altshuler GB, Belikov AV, Erofeev AV. 1996. Comparative study of contact and noncontact operation mode of hard tooth tissues Er-laser processing. 5th International Congress of the International Society of Laser Dentistry, Vol. 21-25 (Jerusalem, Israel, 1996).
- Altshuler GB, Belikov AV, Sinelnik YA. A laser-abrasive method for the cutting of enamel and dentin. *Lasers Surg Med* 2001;28:435-444.
- Majaron M, Sustercic D, Lukac M. 1998. Fiber-tip drilling of hard dental tissues with Er:YAG laser. *Lasers in Dentistry IV*, Vol. 3248:69-77 (SPIE, San Jose, 1998).
- Ith M, Pratisto H, Altermatt HJ, Weber HP. Dynamics of laser-induced channel formation in water and influence of pulse duration on the ablation of biotissue under water with pulsed Er:YAG lasers. *Appl Phys B* 1994;59:621-629.
- Loertscher H, Shi WQ, Grundfest WS. Tissue ablation through water with erbium:YAG lasers. *IEEE Trans Biomed Eng* 1992;39:86-88.
- Forrer M, Ith M, Frenz M, Romano V, Weber HP, Silenok A, Konov VI. 1993. Mechanism of channel propagation in water by pulsed erbium laser radiation. *Laser Interaction With Hard and Soft Tissue*, Vol. 2077:104-112 (SPIE, Budapest, Hungary, 1993).
- Zeck M, Benthin H, Ertl T, Siebert GK, Muller G. 1996. Scanning ablation of dental hard tissue with erbium laser radiation. *Medical Applications of Lasers III*, Vol. 2623:94-102.
- Rechmann P, Glodin DS, Hennig T. 1998. Changes in surface morphology of enamel after Er:YAG irradiation. *Lasers in Dentistry IV*, Vol. 3248:62-68 (SPIE, San Jose, 1998).
- Fried D, Shori R, Duhn C. 1998. Backscattering due to ablative recoil generated during Q-switched Er:YAG ablation of dental enamel. *Lasers in Dentistry IV*, Vol. 3248:78-85 (SPIE, San Jose, CA, 1998).
- Altshuler GB, Belikov AV, Erofeev AV, Skrypnik AV. 1995. Physical aspects of cavity formation of Er-laser radiation. *Lasers in Dentistry*, Vol. 2394:211-222 (SPIE, San Jose, 1995).
- Stern RH, Sognnaes RF, Goodman F. Laser effect on in vitro enamel permeability and solubility. *J Am Dent Assoc* 1966;78:838-843.
- Kuroda S, Fowler BO. Compositional, structural and phase changes in in vitro laser-irradiated human tooth enamel. *Calcif Tissue Int* 1984;36:361-369.
- Fowler B, Kuroda S. Changes in heated and in laser-irradiated human tooth enamel and their probable effects on solubility. *Calcif Tissue Int* 1986;38:197-208.
- Featherstone JDB, Nelson DGA. Laser effects on dental hard tissue. *Adv Dent Res* 1987;1:21-26.
- Konishi N, Fried D, Featherstone JDB, Staninec M. Inhibition of secondary caries by CO<sub>2</sub> laser treatment. *Am J Dent* 1999;12:213-216.
- Young DA, Fried D, Featherstone JDB. 2000. Ablation and caries inhibition of pits and fissures by IR laser irradiation. *Lasers in Dentistry VI*, Vol. 3910:247-253 (SPIE, San Jose, 2000).
- Fried D. 2000. IR ablation of dental enamel. *Lasers in Dentistry VI*, Vol. 3910:136-148 (SPIE, San Jose, 2000).
- Carden A, Morris MD. Application of vibrational spectroscopy to the study of mineralized tissues (review). *J Biomed Optics* 2000;5:259-268.
- Constantz PWB. a.B.: Hydroxyapatite and Related Materials. Boca Raton: CRC Press; 1994.
- Elliot JC. Structure and Chemistry of the Apatites and Other Calcium Orthophosphates. Amsterdam: Elsevier; 1994.
- Featherstone JDB, Pearson S, LeGeros RZ. An IR method for quantification of carbonate in carbonated-apatites. *Caries Res* 1984;18:63-66.
- Featherstone JDB, Fried D, Duhn C. 1998. Surface dissolution kinetics of dental hard tissue irradiated over a fluence range of 1-8 J/cm<sup>2</sup> at a wavelength of 9.3 μm. *Lasers in Dentistry IV*, Vol. 3248:146-151 (SPIE, San Jose, CA, 1998).
- McKinney WR, Hirschmugl CJ, Padmore HA, Lauritzen T, Andresen N, Andronaco G, Patton R, Fong M. 1997. The First Infrared Beamline at the ALS: Design, Construction, and Initial Commissioning. *Accelerator-Based Infrared Sources and Applications*. Vol. 3153:59-67 (SPIE, 1997).
- Fried D, Shori R. 1998. Q-switched Er:YAG ablation of dental hard tissue. 6th International Congress on Lasers in Dentistry, Vol. 77-79 (University of Utah, Maui, Hawaii, 1998).
- Seka W, Fried D, Glana RE, Featherstone JDB. Laser energy deposition in dental hard tissue. *J Dent Res* 1995;74:1086-1092.
- Aminzadeh A, Shahabi S, Walsh LJ. Raman spectroscopic studies of CO<sub>2</sub> laser-irradiated human dental enamel. *Spectrochim Acta A Mol Biomol Spectrosc* 1999;55A:1303-1308.
- Featherstone JDB, Fried D, Bitten E.R. 1997. Mechanism of laser induced solubility reduction of dental enamel. *Lasers in Dentistry III*, Vol. 2973:112-116 (SPIE, San Jose, CA, 1997).
- Shori R, Fried D, Featherstone JDB, Duhn C. 1998. CTE:YAG applications in dentistry. *Lasers in Dentistry IV*, Vol. 3248:86-91 (SPIE, San Jose, CA, 1998).
- Fried D, Zuerlein M, Featherstone JDB, Seka WD, McCormack SM. IR laser ablation of dental enamel: mechanistic dependence on the primary absorber. *Appl Surf Sci* 1997;128:852-856.
- Zuerlein M, Fried D, Featherstone J, Seka W. Optical properties of dental enamel at 9-11 μm derived from time-resolved radiometry. *Spec Top IEEE J Quant Elect* 1999;5:1083-1089.
- Hale GM, Querry MR. Optical constants of water in the 200-nm to 200-μm wavelength region. *Appl Opt* 1973;12:555-562.